Single-frequency Q-switched ring laser with an antiresonant Fabry–Perot saturable absorber

B. Braun and U. Keller

Ultrafast Laser Physics, Institute of Quantum Electronics, Swiss Federal Institute of Technology, ETH Hönggerberg-HPT, CH-8093 Zürich, Switzerland

Received January 3, 1995

We passively Q switched a monolithic Nd:YAG ring laser [monolithic isolated single-mode end-pumped ring laser (MISER)] using an evanescent-wave coupled antiresonant Fabry–Perot saturable absorber. Single-frequency, 0.7-μJ pulses with a pulse width below 100 ns at an $\approx$1-MHz repetition rate are demonstrated. Pulse width and repetition rate can be varied by changing the distance and thus the coupling strength between the crystal and the absorber.

Lasers for optoelectronic applications should be compact, robust, and low maintenance. Monolithic lasers such as a monolithic isolated single-mode end-pumped ring laser[1] (MISER), also called a nonplanar ring oscillator (Fig. 1), and various other approaches[2,3] have been successfully demonstrated and may satisfy the requirements for many industrial applications. For pulse generation, passive techniques that use saturable absorbers have the advantages of simplicity and potentially lower cost. The use of semiconductor saturable absorbers in a device called the antiresonant Fabry–Perot saturable absorber[4,5] (A-FPSA) allows for the design of the relevant parameters for pulse generation, such as absorption wavelength, saturation intensity, impulse response, and insertion loss.[6] Both mode locking and Q switching with an A-FPSA have been successfully demonstrated for many different types of solid-state laser. Passive Q switching of a monolithic laser can be done either by an evanescent-wave-coupled saturable absorber[7] or by direct attachment of an intracavity saturable absorber.[8]

In this Letter we describe the passive Q switching of a cw-pumped single-frequency Nd:YAG MISER by bringing the A-FPSA close to a total-internal-reflection point of the laser cavity. This is to our knowledge the first time that Q switching of a MISER has been demonstrated. Rigidly attaching the nonlinear mirror with fixed spacers would potentially form a compact, quasi-monolithic device (Fig. 1).

The Nd:YAG MISER that we used has an axial mode spacing of 6.0 GHz, a lasing wavelength of 1064 nm, and a geometrical size of approximately 0.2 cm × 1 cm × 1 cm. The resonator is formed inside the crystal by three total-internal-reflection surfaces (B, C, and D; Fig. 1) and a surface A that is coated for high transmission at 809 nm and 2% output coupling at 1064 nm. Applying a magnetic field to the crystal leads to Faraday rotation in YAG,[1] which forces the laser to operate unidirectionally.

By bringing an uncoated nonlinear semiconductor reflector close ($\leq$1 μm) to one of the total-internal-reflection points, we couple light through the evanescent wave into the sample (Fig. 1). The uncoated nonlinear semiconductor reflector is a saturable absorber layer with a thickness d of 0.6 μm grown on a GaAs/AlAs dielectric mirror. The saturable absorber band gap is designed for 1.06 μm and consists of 50 pairs of InGaAs/GaAs multiple quantum wells grown by molecular-beam epitaxy at low temperature (300–400 °C), which results in a carrier recombination time $\tau_c \approx 40$ ps.[6] We measured a saturation fluence of the antireflection-coated sample of $E_{\mathrm{sat}}^0 \approx 50\ \mu\mathrm{J/cm}^2$, using 1.4-ps-long pulses from a mode-locked Ti:sapphire laser.[6] However, because the carrier lifetime is much shorter than the Q-switched pulse duration of $\approx$100 ns, the saturation power $P_{\mathrm{sat}}^0 = (E_{\mathrm{sat}}^0/\tau_c)\,A \approx 375$ W and the evanescent-wave coupling will determine only the onset of passive Q switching. The laser mode area A inside the MISER is $\approx 3 \times 10^{-4}$ cm^2.

The nonlinear reflector combined with the total internal reflection from the MISER acts similarly to an intracavity A-FPSA, except that the amount of light coupled into the device is determined by the evanescent wave, not by the dielectric top reflector. The nonnormal incidence reduces the finesse of the device. However, the A-FPSA performance is not significantly degraded because the saturable absorber is not strongly bleached and the low-Q Fabry–Perot saturable absorber is operated at antiresonance. The reflectivity of the equivalent top mirror of the evanescent-wave-coupled A-FPSA changes exponentially with the distance z between

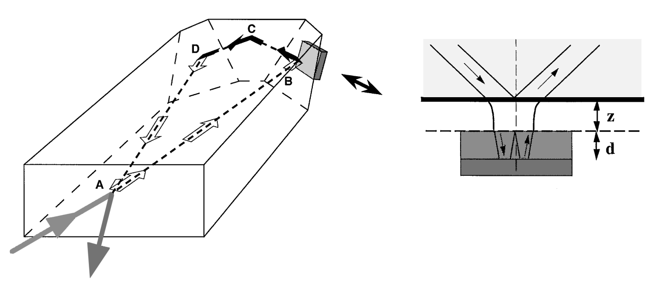

Fig. 1. Layout of the MISER with an A-FPSA coupled to a total-internal-reflection point and (at the right) a schematic of the interface between the MISER and the A-FPSA.

0146-9592/95/091020-03$6.00/0

the crystal interface and the device. The antiresonance condition is obtained by adjusting the absorber thickness d accordingly.[6] Antiresonance is still required if one is to minimize the nonsaturable insertion loss and reduce any heating effects. Thus no temperature control is required and we simply indium solder the device onto a copper holder. An antireflection-coated saturable absorber gives typically a low-intensity reflectivity of ≈50%, which gives an intensity absorption coefficient of 5800 cm^{-1}. Using transmission matrix methods we then can calculate the low-intensity reflectivity R_B at the surface B as a function of the spacing z (Fig. 2). In analogy to the A-FPSA we can determine an effective saturation power of $P_{sat}^{eff} = P_{sat}^{0}/\xi$, with the ξ factor given in Fig. 2.[6] The effective saturation power determines the threshold for stable passive Q switching.

For the proof of principle, we pumped the laser with a cw Ti:sapphire laser at 809 nm, polarized parallel to the crystal plane to minimize reflection losses at the front surface. The pump radius was measured to be 33 μm. A diode-pumped MISER has been demonstrated before and is available as a commercial product. Because we wish to vary the coupling between the MISER and the saturable absorber by varying the distance z, and because the device must be very close (<1 μm) and parallel to the crystal, we polished a new surface at the crystal edge facing surface B (Fig. 1). This permitted optical access with a He–Ne laser beam for interferometric alignment of the saturable absorber with respect to the crystal facet. We then mounted the saturable absorber on a five-axis piezo-controlled translation stage with a resolution of ±50 nm. However, for potential applications requiring fixed operating parameters of the laser, the sample could be rigidly attached to the crystal, for example, by a fixed semiconductor spacer grown on the saturable absorber device or by application of a low-index film between the absorber and the crystal. For the modified MISER we measured a cw slope efficiency of 48% with a pump threshold of 170 mW, corresponding to a total cavity loss of 3.1%, where a 2% loss is due to the output coupler.

The threshold for Q switching was observed at a cw pump power of 790 mW and an average intracavity power of 5.6 W with the semiconductor saturable absorber placed at a distance $z \approx 0.3$ μm, estimated by the additional intracavity losses (Fig. 2). This distance gives a ξ factor of 0.046 (Fig. 2), an effective saturation power $P_{sat}^{eff} = P_{sat}^{0}/\xi \approx$ 8.1 kW, an additional intracavity loss of ≈2.7% (Fig. 2), and an equivalent A-FPSA top reflector $R_t = 87\%$, which gives an unsaturated but maximal saturable amplitude loss modulation $q_0 \approx 1\%$.[6] The round-trip small-signal gain G_0 was 170%, which was determined with the measured relaxation oscillation of the cw pumped MISER with a cavity round-trip time $T_R = 167$ ps, a laser upper-state lifetime $\tau_L = 230$ μs, and a total cavity loss of 3.1%.[9] This gives a pump parameter $r = \ln G_0/l_0 \approx 9.1$, where l_0 is the total intracavity loss coefficient given by 0.031 plus 0.027. The pump parameter describes how many times above threshold the laser operates. The threshold condition for passive Q switching is given by[8,10,11]

$$-T_L P \frac{dq}{dP}\bigg|_{cw} = \frac{T_L q_0}{\chi} \frac{r-1}{\left(1+\dfrac{r-1}{\chi}\right)^2}. \qquad (1)$$

For $\chi \gg r - 1$, Eq. (1) is reduced to

$$\frac{T_L q_0}{\chi} \frac{(r-1)}{r} > 1, \qquad (2)$$

where $T_L = \tau_L/T_R \approx 1.4 \times 10^6$ is the laser upper-state lifetime normalized to the round-trip time and $\chi = P_{sat}^{eff}/P_L$, with P_L the saturation power of the gain medium. In our case we have $P_L = Ah\nu/\sigma\tau_L \approx$ 0.63 W and therefore $\chi = 1.3 \times 10^4$. Because

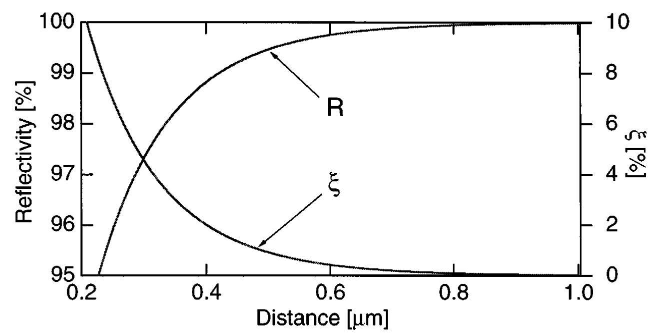

Fig. 2. Calculated reflectivity R_B and the ξ factor as functions of the spacing z between the crystal and the absorber. The thickness of the absorber is set to antiresonance, and the effective saturation intensity is given by $I_{sat}^{eff} = I_{sat}^{0}/\xi$, where I_{sat}^{0} is the saturation intensity of the antireflection-coated saturable absorber.

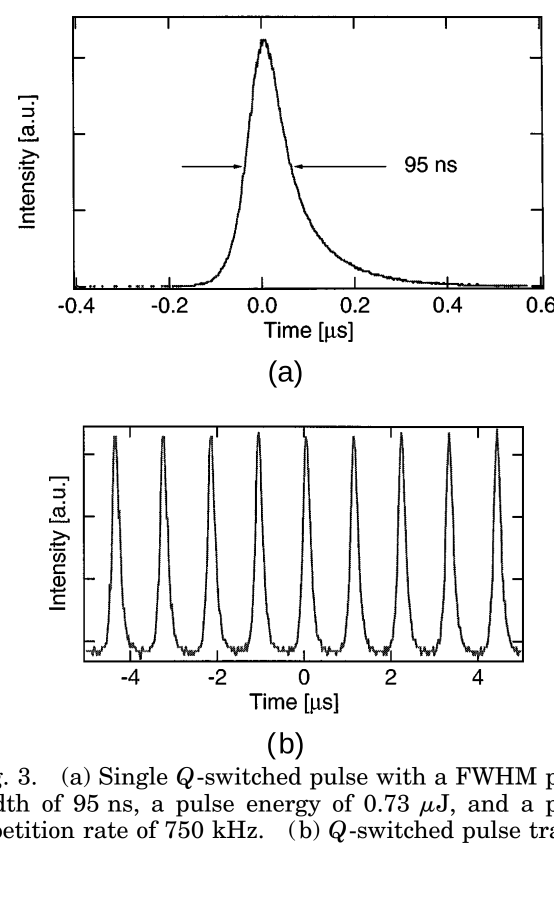

Fig. 3. (a) Single Q-switched pulse with a FWHM pulse width of 95 ns, a pulse energy of 0.73 μJ, and a pulse repetition rate of 750 kHz. (b) Q-switched pulse train.

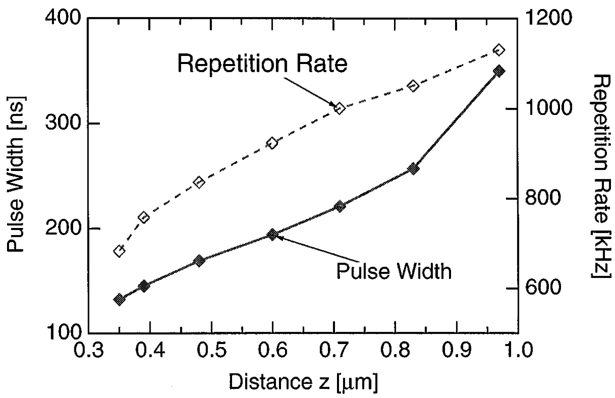

Fig. 4. Pulse width and repetition rate as functions of the spacing between the crystal and the semiconductor device ($P_{\mathrm{pump}} = 2$ W).

$\chi \gg 1$, our calculations are in accord with relation (2). For our experimental threshold of Q switching we obtain a value of 0.96 for the left-hand side of relation (2), which is in excellent agreement with the theoretical prediction for the threshold of Q switching. One can easily design the saturable absorber for a lower Q-switching threshold by using a smaller $P_{\mathrm{sat}}^{\mathrm{eff}}$ with, for example, a larger carrier lifetime without increasing the intracavity loss.

At a pump power of 3.1 W and an average output power of 545 mW, we obtained single-frequency TEM_{00} Q-switched pulses as short as 95 ns with a repetition rate of 750 kHz and a pulse energy of 0.73 μJ [Fig. 3(a)]. The intracavity peak power at the reflecting surface B is then 360 W, which is still well below the effective saturation power $P_{\mathrm{sat}}^{\mathrm{eff}}$ of 8.1 kW. Above 3.1 W of pump power it became more difficult to maintain unidirectional lasing, and no stable Q switching was observed with counter-propagating laser beams. Figure 3(b) shows that over a time duration of 10 consecutive pulses the peak-to-peak intensity fluctuations is less than 2% and the peak-to-peak timing jitter is below 1% (i.e., integrated intensity noise and timing jitter over a frequency span from 75 kHz to 500 MHz). The long-term stability observed over hours was very good. Single-frequency output was determined with both a scanning Fabry–Perot interferometer and a high-frequency microwave spectrum analyzer. The measured bandwidth was limited by the resolution of the Fabry–Perot interferometer (0.004 nm), and no additional axial modes were observed spaced at the axial mode spacing at the axial mode spacing of 0.023 nm and their integer multiples. As a further confirmation, we did not observe any axial mode-beating signals on the microwave spectrum analyzer at the axial mode spacing of 6.0 GHz and integer multiples as high as 18 GHz.

By changing the distance of the evanescent-wave-coupled saturable absorber, we can vary the effective saturation power $P_{\mathrm{sat}}^{\mathrm{eff}} = P_{\mathrm{sat}}^{0}/\xi$ (Fig. 2) and therefore the pulse repetition rate and the pulse duration (Fig. 4). With a distance variation of 0.6 μm the pulse width changes from approximately 100 to 350 ns and the repetition rate changes from 700 kHz to 1.2 MHz.

In summary, using evanescent-wave coupling in a semiconductor saturable absorber device, we demonstrated a simple but flexible technique to Q switch a monolithic laser. This approach does not depend on a specific geometry or gain material but can be applied to other monolithic lasers and different wavelengths by adjustment of the parameters of the sample. That makes it an interesting alternative to other saturable absorbers such as Cr^{4+}-doped crystals.[12] Good stability in terms of amplitude and frequency fluctuations, the extremely narrow lasing linewidth, and the compact and robust design make this an interesting device for applications such as lidar systems and nonlinear optics.

We thank T. J. Kane of Lightwave Electronics for supplying the MISER crystal, T. H. Chiu of AT&T Bell Laboratories for growing the semiconductor saturable absorber, J. Hajfler of ETH Zürich for polishing the modified laser crystal, the group of J. Mlynek for helpful discussions, and the support of the Swiss priority program in optics.

References

1. T. J. Kane and R. L. Byer, Opt. Lett. **10,** 65 (1985).
2. J. J. Zayhowski and C. Dill III, Opt. Lett. **17,** 1201 (1992).
3. K. Fiedler, S. Schiller, R. Paschotta, P. Kürz, and J. Mlynek, Opt. Lett. **18,** 1786 (1993).
4. U. Keller, D. A. B. Miller, G. D. Boyd, T. H. Chiu, J. F. Ferguson, and M. T. Asom, Opt. Lett. **17,** 505 (1992).
5. U. Keller, Appl. Phys. B **58,** 347 (1994).
6. L. R. Brovelli, U. Keller, and T. H. Chiu, J. Opt. Soc. Am. B **12,** 311 (1995).
7. B. Braun and U. Keller, in *Conference on Lasers and Electro-Optics,* Vol. 8 of 1994 OSA Technical Digest Series (Optical Society of America, Washington, D.C., 1994), paper CPD20.
8. B. Braun, F. X. Kärtner, U. Keller, J.-P. Meyn, G. Huber, and T. H. Chiu, in *Digest of Conference on Advanced Solid-State Lasers* (Optical Society of America, Washington, D.C., 1995), paper ThB1.
9. K. J. Weingarten, B. Braun, and U. Keller, Opt. Lett. **19,** 1140 (1994).
10. H. A. Haus, IEEE J. Quantum Electron. **QE-12,** 169 (1976).
11. F. X. Kärtner, L. R. Brovelli, D. Kopf, M. Kamp, I. Calasso, and U. Keller, "Control of solid-state laser dynamics by semiconductor devices," Opt. Eng. (to be published), Eq. II.6.
12. S. Zhou, K. K. Lee, Y. C. Chen, and S. Li, Opt. Lett. **18,** 511 (1993).